Structure−Morphology−Electroluminescence Relationship for Hybrid Conjugated Polymers

Liming Ding,[†] Zhixiang Lu,[†] Daniel A. M. Egbe,[‡] and Frank E. Karasz*,[†]

Department of Polymer Science and Engineering, University of Massachusetts, Amherst, Massachusetts 01003, and Institut für Organische Chemie und Makromolekulare Chemie der Friedrich-Schiller Universität Jena, Humboldtstrasse 10, D-07743 Jena, Germany

Received July 19, 2004; Revised Manuscript Received October 5, 2004

ABSTRACT: A comparative study of a series of conjugated polymers is described. The solution absorption spectra of polymers **1**−**3** show unusual red shifts relative to their film spectra, which is due to strong aggregate formation in the concentrated solution. The polymer with octadecyloxy side chains shows improved LED performance because of increased solubility, film-forming capability, and optimized film morphology. The long side chains are also capable of forming small insulating domains which inhibit exciton interchain migration thereby enhancing exciton confinement and EL efficiency. 2-Ethylhexyloxy side chains also favor exciton confinement due to their increased steric hindrance to interaction between neighboring conjugated main chains. AFM and contact angle measurements indicate that polymer film surface properties are controlled by polymer backbone structure and by the length, geometry, and polarity of the side group. The polymer film surface morphology affects the local electrical field distribution within the LED, electron injection/transport at the polymer/Ca interface, and overall it influences the device performance.

Introduction

Phenylene ethynylene oligomers and polymers (PPE) attract wide interest.[1−6] Studies of molecular packing,[1d] energy migration,[2b] polarized photoluminescence,[2d] chromophore aggregation[3b] and charge carrier mobility[4c] in these materials have been carried out. PPEs are highly fluorescent materials with high quantum yields which are probably due to their rigid structure which limits potential nonradiative deactivation pathways.[2a] Poly(*p*-phenylene ethynylene)s have been used as the emitting layers in LEDs.[7] PV/PE hybrid copolymers having both carbon−carbon double and triple bonds are candidate materials for optoelectronic application as they combine the high fluorescence quantum yields of PPE with the chemical stability of PPV.[8] Bunz et al.,[9] Egbe et al. [10] and Pang et al.[11a] incorporated acetylene bonds (−C≡C−) into a PPV backbone to make numerous hybrid phenylenevinylene/phenylene ethynylene (PV/PE) materials with novel structures and interesting properties. Jeglinski et al.[12] first reported LEDs based on 2,5-dialkoxy substituted poly(*p*-diethynylene-phenylene-*p*-diphenylenevinylene). More recently, we have obtained efficient LEDs from alkoxy substituted PV/PE copolymer materials.[11] A PV/PE hybrid conjugated polymer with pendant fullerenes has been used as the active layer of a photovoltaic cell.[13]

In this contribution, we report the thin film properties of a series of PE/PV hybrid conjugated polymers bearing alkoxy side chains and CN groups (Figure 1). The effect of side chains on the photophysical and optoelectronic properties has been studied, and the surface and morphology of spin-coated films have been investigated by measuring contact angles and observing AFM images.

* Corresponding author. E-mail: fekarasz@polysci.umass.edu.
[†] University of Massachusetts.
[‡] Institut für Organische Chemie und Makromolekulare Chemie der Friedrich-Schiller Universität Jena.

Results and Discussion

The morphology of films of polymer **1**−**5** on silicon substrates spin-coated from chloroform solutions was studied by AFM in the tapping mode. The AFM height and phase images (2 μm × 2 μm) are shown in Figure 2 with RMS roughness data listed in Table 1. The roughness for films **1**−**5** are 0.521, 0.445, 0.407, 0.559, and 0.585 nm, respectively. With the same solution concentration and spinning speed, the morphology of the spin-coating films was affected by the solvent−solute interaction between the polymer and chloroform, though all solutions are homogeneous. If the compatibility between the polymer and chloroform is poor, the polymer readily precipitates and forms a film with a considerable roughness. Polymer **3** provided the smoothest film because of the presence of the two longer octadecyloxy side chains which improve its solubility in chloroform. The branched 2-ethylhexyloxy side chains interact with chloroform somewhat better than do the octyloxy side chains; therefore the **2** film is seen to be smoother than that of **1**. Film **4** shows a higher roughness because the repeating unit of **4** lacks four alkoxy side chains compared with polymers **1**−**3**. The polarity of the CN group is higher than chloroform, which decreases the compatibility between **4** and this solvent; therefore, **4** precipitates quickly, leading to a rougher film. Finally, for polymer **5** containing a pure phenylenevinylene backbone, even though the main chain is much softer than that of the hybrid materials **1**−**4** containing the rigid phenylene ethynylene units, and there are also comparable grafted alkoxy side chains, where the material yields the roughest spin-coating film because of the high grafting density of polar CN groups.

Contact angles give a measure of the interaction between the probe fluid and the polymer film surface. Water contact angles for films **1**−**5** are big and close (θ_A/θ_R = ∼108°/∼88°, see Table 1), indicating that all the film surfaces are hydrophobic. In contrast, hexadecane shows very low contact angles, since hexadecane

10.1021/ma040124m CCC: $27.50
Published on Web 12/04/2004

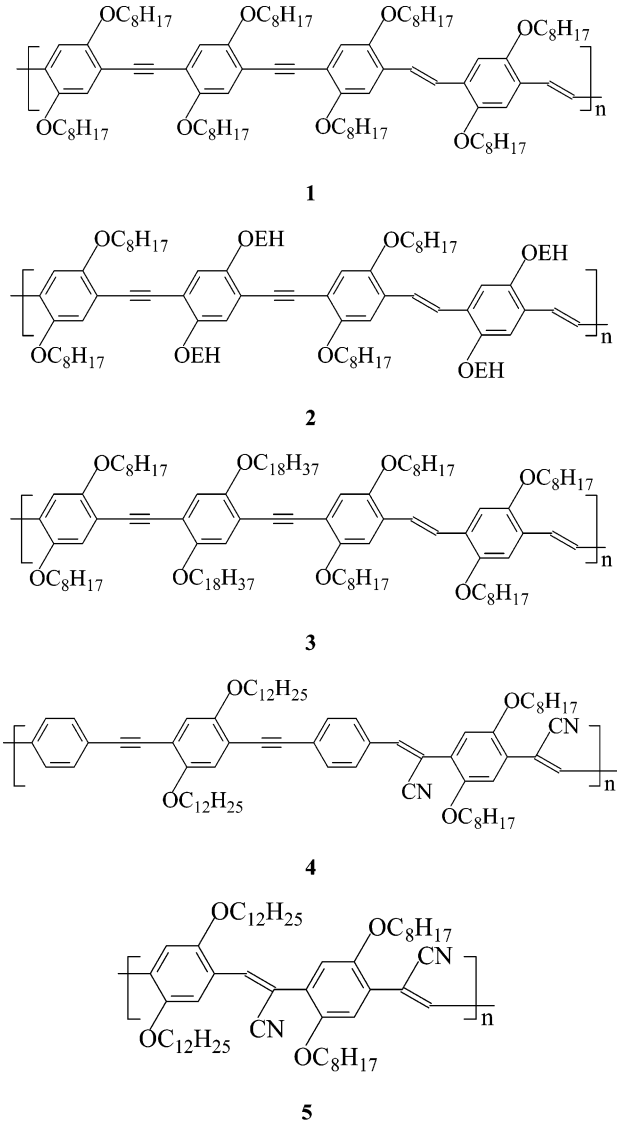

Figure 1. Chemical structures of polymers **1**−**5**.

can interact with the alkoxy side chains on film surface. The contact angles are 18°/8°, 24°/9°, 19°/9°, 13°/8°, and 15°/7° for films **1**−**5** respectively. Hexadecane has the lowest contact angle on film **4**, because the **4** backbone is more accessible and hexadecane can easily penetrate. Hexadecane presents the highest contact angle on film **2**, because the branched 2-ethylhexyloxy side chains might cause hexadecane penetration to be a little bit more difficult.

The absorption, PL, and EL spectra of the polymers are shown in Figure 3, Figure 4, and Figure 5, respectively. The concentration of polymer/chloroform solutions is 0.05 mg/mL. Spin-coating films are used to obtain solid-state spectra. LEDs were made using the configuration, ITO/PEDOT/polymer/Ca. The photophysical data and device characteristics are summarized in Table 2. The solution absorption peak wavelengths are 470, 471, 472, 418, and 463 nm for polymers **1**−**5** respectively. Compared with film absorption spectra, the solution spectra of polymers **1**−**3** show unusual red shifts. This might be due to the remarkable aggregate formation in concentrated solution of polymers **1**−**3.** The absorption of **4** film displays a ∼40 nm red shift because of the presence of the conjugated and electron-with-

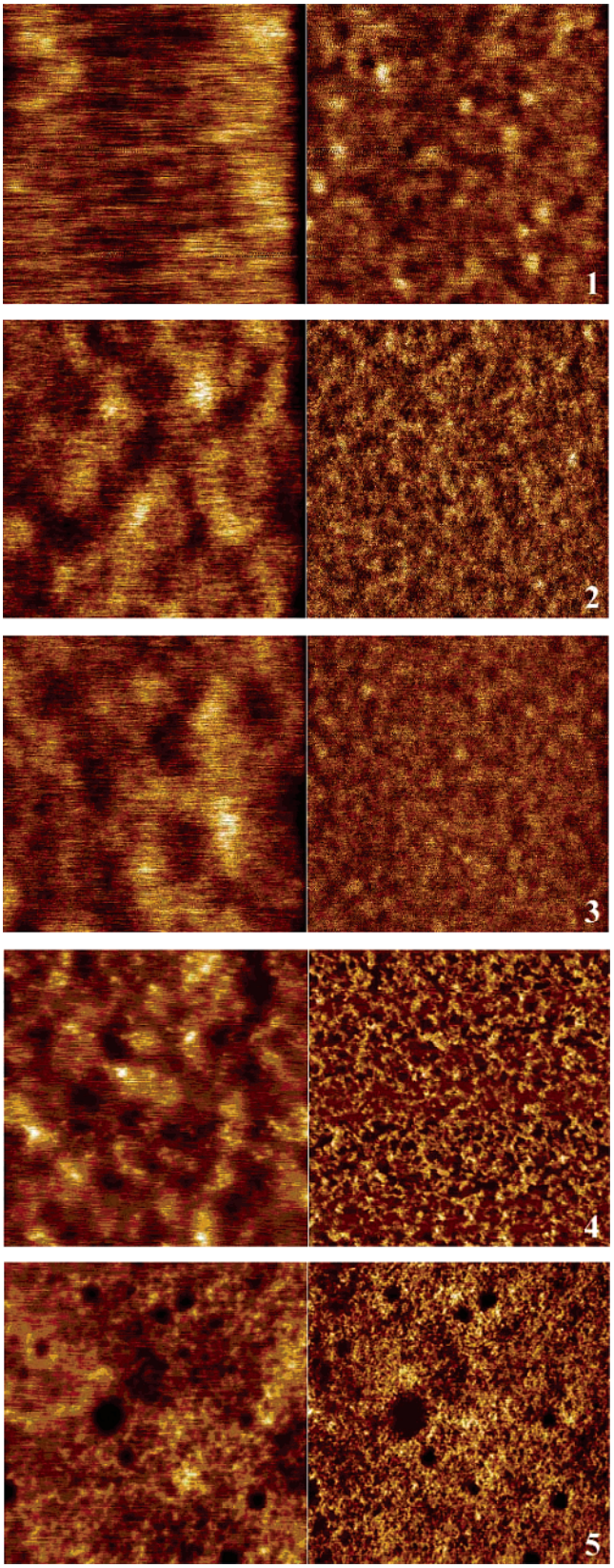

Figure 2. AFM images of polymer films **1**−**5**.

drawing CN groups. Polymer **5** shows a greater red shift (∼100 nm) because of the dense CN grafting on the main chain. The absence of carbon−carbon triple bond in **5** may also contribute to the greater red shift. The solution PL peak wavelengths are 523, 524, 521, 496, and 550 nm for polymers **1**−**5** respectively. The film PL spectra show red shifts because of chain packing which could

Table 1. Roughness and Contact Angles for the Polymer Films

polymer	RMS roughness (nm)	contact angle, θ_A/θ_R (deg) water	hexadecane
1	0.521	109/88	18/8
2	0.445	110/87	24/9
3	0.407	107/91	19/9
4	0.559	107/83	13/8
5	0.585	107/91	15/7

extend the conjugation. Excimer formation may also contribute to this shift. The PL spectra of polymer **4** show blue shifts compared to **1**−**3**, which is due to lower grafting content of alkoxy side chains. The Stokes shifts of **1**−**5** films are 179, 169, 178, 110, and 127 nm, respectively. The film absorption spectrum of **2** showed a shoulder which might be attributed to n−π^* transition. Presence of this weak n−π^* transition could be responsible for the observation that the absorption peak of the **4** film occurs at a longer wavelength than that of **1**−**3**, while the emission peak of the **4** film is at a shorter wavelength.

LEDs made from polymers **1**−**3** emit yellow-green light. Comparing EL spectra of **1**−**3** with their respective PL spectra, it is noteworthy that all EL spectra present vibronic fine structures. This is due to the different exciton generation process in PL and EL. Device **4** also emits yellow-green light. The band gap

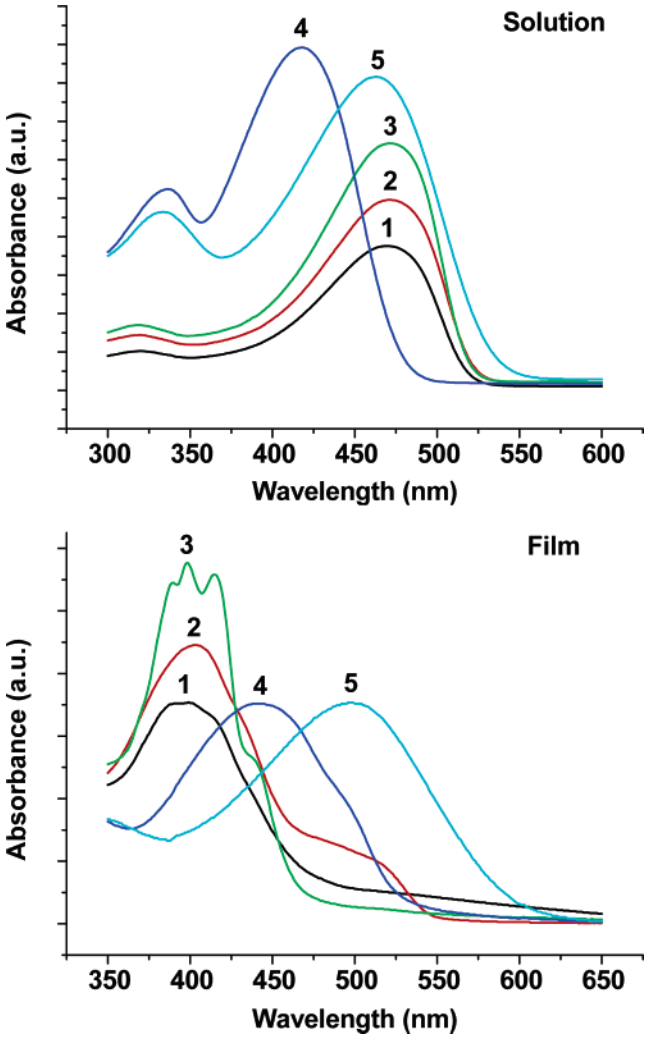

Figure 3. Absorption spectra for polymers **1**−**5**.

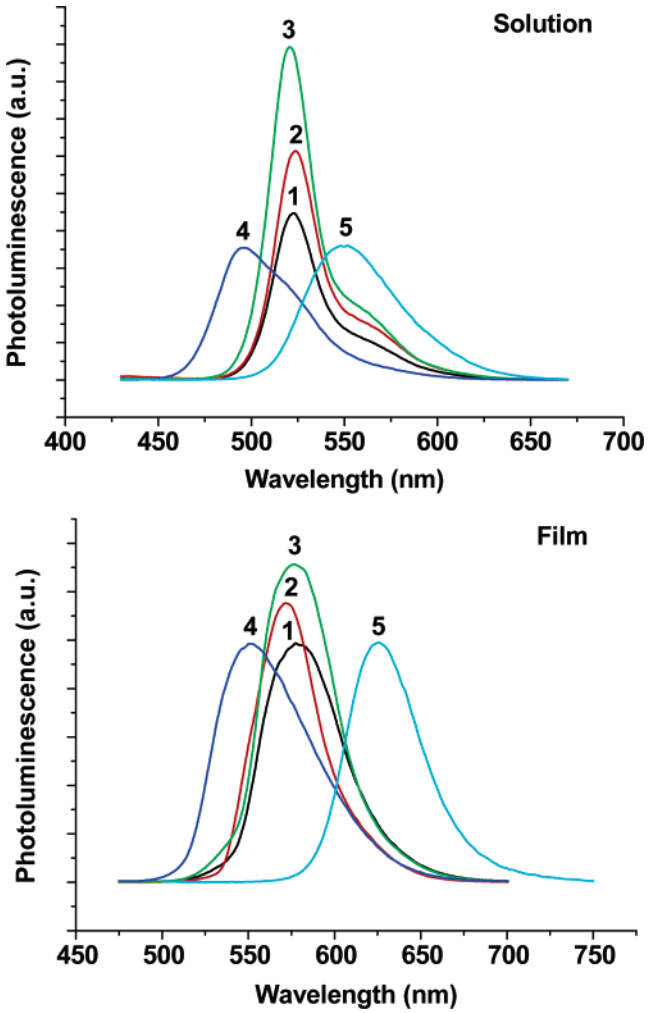

Figure 4. PL spectra for polymers **1**−**5**.

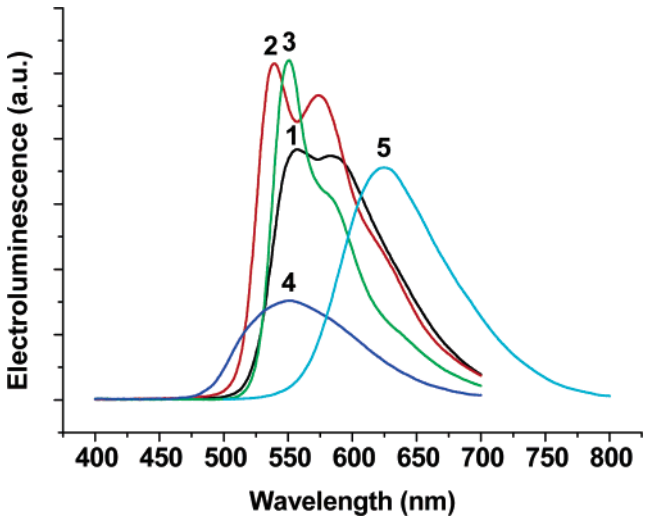

Figure 5. EL spectra for polymers **1**−**5**.

increase resulting from the absence of four alkoxy side chains on the repeating unit is compensated by the addition of two cyano groups. Device **5** emits pure orange light at 624 nm with a ~70 nm red shift compared with the other four devices which can be attributed to the lower band-gap phenylenevinylene backbone and the high density of CN substituent. Figure 6 shows the voltage dependence of EL spectra for polymers **2** and **3**. With the increase of bias voltage, the

Table 2. Photophysical Properties of the Polymer Films and LED Characteristics

polymer	λ_{max}^{Abs} (nm)	λ_{max}^{PL} (nm)[a]	band gap (eV)[b]	λ_{max}^{EL} (nm)[c]	turn-on voltage(V)[d]	LE (cd/A)[e]	QE_{ext}[f] (%)
1	399	578	2.29	**557**, 583	10	0.064	1.44×10^{-2}
2	403	572	2.31	**539**, 573	6.5	0.96	0.22
3	398	576	2.37	**551**, 583	6	4.4	0.98
4	441	551	2.39	551	8.5	0.31	6.92×10^{-2}
5	498	625	2.10	624	10.5	0.17	0.13

[a] Excitation wavelength 380 nm. [b] The band gap was obtained from the point at which the normalized absorption and emission spectra intersect. [c] Boldface data indicates the major peak. [d] The turn-on voltage is defined as the voltage at which the luminance starts to increase rapidly. [e] Maximum luminous efficiency. [f] Maximum external quantum efficiency.

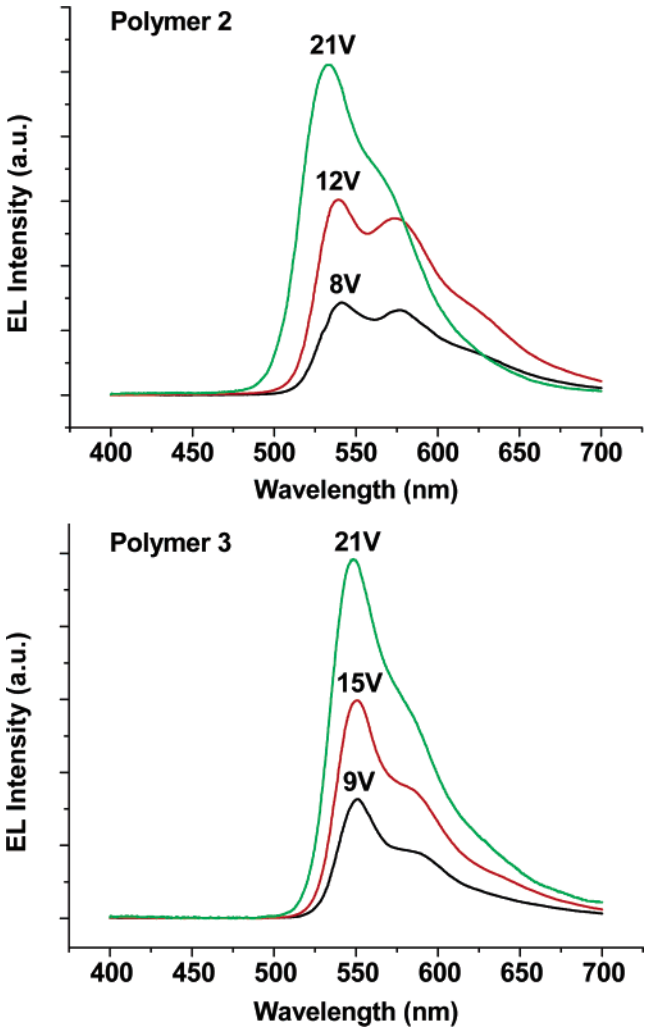

Figure 6. Voltage dependence of EL spectra.

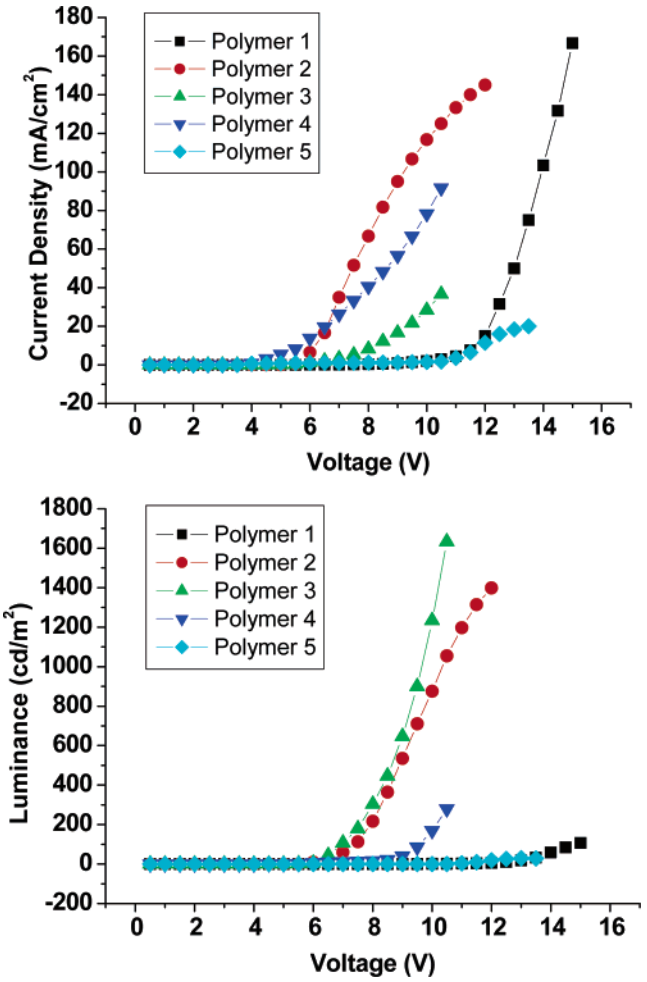

Figure 7. Current density vs voltage and luminance vs voltage characteristics for devices ITO/PEDOT/polymer/Ca.

EL emission shows a blue shift and the relative intensity of the 0−0 band increases and finally dominates the spectra. This is due to Joule heating in the LEDs at high current;[14] a band gap distribution in the materials may also contribute to the shift. Figure 7 shows the current density−voltage−luminance characteristics for the five LEDs. The turn-on voltages for devices **1**−**5** are 10, 6.5, 6, 8.5, and 10.5 V, respectively. The maximum external quantum efficiencies reach 1.44×10^{-2}%, 0.22%, 0.98%, 6.92×10^{-2}% and 0.13% respectively. It is seen that when two octyloxy side chains are replaced with two octadecyloxy side chains, the EL efficiency greatly increases (**3** vs **1**). The longer octadecyloxy side chains improve polymer solubility, film-forming capability, and film morphology which affects the device performance. In addition, longer side chains might form small insulating domains which inhibit exciton interchain migration enhancing exciton confinement and EL efficiency. Our previous study[15] indicates that polymers with 2-ethylhexyloxy side chains are more efficient than those with octyloxy side chains. In this work, device **2** shows a higher efficiency than device **1**, conforming with previous results. 2-Ethylhexyloxy side chains are more favorable for exciton confinement due to their steric hindrance to interaction between neighboring conjugated main chains. Polymers **4** and **5** display higher turn-on voltages and lower quantum efficiencies than do polymers **2** and **3**. CN groups let them precipitate quickly from chloroform solution, leading to the formation of pinholes (see AFM images of film **5**) which may cause shorts during device operation. In addition, the strong interchain interaction in **4** and **5** increases the probability of interchain exciton quenching which can deteriorate device performance.

It should be noted that the present LED data for polymers **4** and **5** can be compared with results for similar systems shown in ref 16. In the latter the

respective films were cast from chlorobenzene solution (private communication; see also Supporting Information for ref 16) whereas in the present work a chloroform solvent was used. We attributed the lower luminous efficiencies given in ref 16 for polymers **4** and **5** to the differences in film morphology attributable to film preparation from the differing solvents.

In conclusion, we studied a series of conjugated polymers with or without triple bond, with or without CN groups. AFM and contact angle measurements indicate that polymer film surface properties are controlled by polymer backbone structure, side group nature (length, geometry and polarity). The polymer film surface morphology will affect the local electrical field distribution in the LED, electron injection/transport at the polymer/Ca interface, and finally affect device performance. Photophysical properties of these polymers in solution or in solid state strongly correlate with their structures.

Experimental Section

Materials and Characterization. Polymers **1**−**5** were synthesized according to procedures described previously.[10c,10e,16] Silicon wafers (International Wafer Service) were characterized by 100 orientation, P/B doping, 20−40 Ω·cm resistivity, 450−575 μm thickness. The thickness of the native oxide on these wafers was determined to be ~22 Å by ellipsometry. The wafers were cut into 1.2 cm × 1.2 cm squares, washed by reverse osmosis (RO) water, blown dry by compressed air, and cleaned by O_2 plasma. The silicon wafers were used immediately after 5 min cleaning in the plasma chamber at 100 milliTorr. House-purified water (reverse osmosis) was further purified using a Millipore Milli-Q system with reverse osmosis, ion-exchange, and filtration steps (1.8×10^7 Ω·cm). Hexadecane (anhydrous) (Aldrich) was used as received. Contact angle measurements were made with a Ramé-Hart telescopic goniometer and a Gilmont syringe with a 24-gauge flat-tipped needle. Dynamic advancing (θ_A) and receding angles (θ_R) were recorded as the probe fluid was added to and withdrawn from the drop, respectively. The values reported are averages of three to five measurements made on different areas of the sample surfaces. All samples exhibited contact angles within ± 1° of the average value reported herein. AFM images were obtained from a Digital Instruments Dimension 3100 scanning probe microscope operated in the tapping mode. UV−vis spectra were recorded on a HITACHI U-3010 UV/vis spectrophotometer. PL spectra were recorded on a Perkin-Elmer LS 50B luminescence spectrometer.

LED Fabrication and Measurements. In fabrication of LED devices, PEDOT/PSS (Bayer Co.) was spin-cast directly onto ITO glass, and polymer solutions (10 mg/mL in chloroform) filtered through 0.2 μm Millex-FGS Filters (Millipore Co.) were spin-cast onto the dried PEDOT/ITO substrates under a nitrogen atmosphere. Calcium electrodes of 400 nm thickness were evaporated onto the polymer films at about 10^{-7} Torr, followed by a protective coating of aluminum. The electroluminescent properties of the LEDs sealed in argon were characterized using a custom-made system described previously.[17]

Acknowledgment. L.D. and F.E.K. wish to thank the AFOSR for generous support.

References and Notes

(1) (a) Prince, R. B.; Saven, J. G.; Wolynes, P. G.; Moore, J. S. *J. Am. Chem. Soc.* **1999**, *121*, 3114. (b) Lahiri, S.; Thompson, J. L.; Moore, J. S. *J. Am. Chem. Soc.* **2000**, *122*, 11315. (c) Brunsveld, L.; Meijer, E. W.; Prince, R. B.; Moore, J. S. *J. Am. Chem. Soc.* **2001**, *123*, 7978. (d) Kubel, C.; Mio, M. J.; Moore, J. S.; Martin, D. C. *J. Am. Chem. Soc.* **2002**, *124*, 8605.

(2) (a) Swager, T. M.; Gil, C. J.; Wrighton, M. S. *J. Phys. Chem.* **1995**, *99*, 4886. (b) Levitsky, I. A.; Kim, J.; Swager, T. M. *J. Am. Chem. Soc.* **1999**, *121*, 1466. (c) Kim, J.; Levitsky, I. A.; McQuade, D. T.; Swager, T. M. *J. Am. Chem. Soc.* **2002**, *124*, 7710. (d) Breen, C. A.; Deng, T.; Breiner, T.; Thomas, E. L.; Swager, T. M. *J. Am. Chem. Soc.* **2003**, *125*, 9942.

(3) (a) Kloppenburg, L.; Song, D.; Bunz, U. H. F. *J. Am. Chem. Soc.* **1998**, *120*, 7973. (b) Levitus, M.; Schmieder, K.; Ricks, H.; Shimizu, K. D.; Bunz, U. H. F.; Garcia-Garibay, M. A. *J. Am. Chem. Soc.* **2001**, *123*, 4259. (c) Wilson, J. N.; Steffen, W.; McKenzie, T. G.; Lieser, G.; Oda, M.; Neher, D.; Bunz, U. H. F. *J. Am. Chem. Soc.* **2002**, *124*, 6830. (d) Erdogan, B.; Song, L.; Wilson, J. N.; Park, J. O.; Srinivasarao, M.; Bunz, U. H. F. *J. Am. Chem. Soc.* **2004**, *126*, 3678.

(4) (a) Weder, C.; Wagner, M. J.; Wrighton, M. S. *Mater. Res. Soc. Sym. Proceedings* **1996**, *413*, 77. (b) Huber, C.; Bangerter, F.; Caseri, W. R.; Weder, C. *J. Am. Chem. Soc.* **2001**, *123*, 3857. (c) Kokil, A.; Shiyanovskaya, I.; Singer, K. D.; Weder, C. *J. Am. Chem. Soc.* **2002**, *124*, 9978.

(5) (a) Li, J.; Pang, Y. *Macromolecules* **1998**, *31*, 5740. (b) Chu, Q.; Pang, Y. *Macromolecules* **2003**, *36*, 4614. (c) Li, J.; Pang, Y. *Synth. Met.* **2004**, *140*, 43.

(6) (a) Arnt, L.; Tew, G. N. *J. Am. Chem. Soc.* **2002**, *124*, 7664. (b) Breitenkamp, R. B.; Tew, G. N. *Macromolecules* **2004**, *37*, 1163. (c) Arnt, L.; Tew, G. N. *Macromolecules* **2004**, *37*, 1283.

(7) (a) Swanson, L. S.; Shinar, J.; Ding, Y. W.; Barton, T. J. *Synth. Met.* **1993**, *55*, 1. (b) Montali, A.; Smith, P.; Weder, C. *Synth. Met.* **1998**, *97*, 123. (c) Pschirer, N. G.; Miteva, T.; Evans, U.; Roberts, R. S.; Marshall, A. R.; Neher, D.; Myrick, M. L.; Bunz, U. H. F. *Chem. Mater.* **2001**, *13*, 2691. (d) Chu, Q.; Pang, Y.; Ding, L.; Karasz, F. E. *Macromolecules* **2002**, *35*, 7569.

(8) Schenning, A. P. H. J.; Tsipis, A. C.; Meskers, S. C. J.; Beljonne, D.; Meijer, E. W.; Brédas, J. L. *Chem. Mater.* **2002**, *14*, 1362.

(9) (a) Brizius, G.; Pschirer, N. G.; Steffen, W.; Stitzer, K.; zur Loye, H.-C.; Bunz, U. H. F. *J. Am. Chem. Soc.* **2000**, *122*, 12435. (b) Wilson, J. N.; Windscheif, P. M.; Evans, U.; Myrick, M. L.; Bunz, U. H. F. *Macromolecules* **2002**, *35*, 8681. (c) Wilson, J. N.; Josowicz, M.; Wang, Y.; Bunz, U. H. F. *Chem. Commun.* **2003**, 2962.

(10) (a) Egbe, D. A. M.; Tillmann, H.; Birckner, E.; Klemm, E. *Macromol. Chem. Phys.* **2001**, *202*, 2712. (b) Egbe, D. A. M.; Birckner, E.; Klemm, E. *J. Polym. Sci., Polym. Chem.* **2002**, *40*, 2670. (c) Egbe, D. A. M.; Roll, C. P.; Birckner, E.; Grummt, U.-W.; Stockmann, R.; Klemm, E. *Macromolecules* **2002**, *35*, 3825. (d) Egbe, D. A. M.; Roll, C. P.; Klemm, E. *Des. Monomers Polym.* **2002**, *5*, 245. (e) Egbe, D. A. M.; Bader, C.; Nowotny, J.; Günther, W.; Klemm, E. *Macromolecules* **2003**, *36*, 5459.

(11) (a) Chu, Q.; Pang, Y.; Ding, L.; Karasz, F. E. *Macromolecules* **2003**, *36*, 3848. (b) Egbe, D. A. M.; Bader, C.; Klemm, E.; Ding, L.; Karasz, F. E.; Grummt, U.-W.; Birckner, E. *Macromolecules* **2003**, *36*, 9303.

(12) Jeglinski, S. A.; Amir, O.; Wei, X.; Vardeny, Z. V.; Shinar, J.; Cerkvenik, T.; Chen, W.; Barton, T. J. *Appl. Phys. Lett.* **1995**, *67*, 3960.

(13) Ramos, A. M.; Rispens, M. T.; van Duren, J. K. J.; Hummelen, J. C.; Janssen, R. A. J. *J. Am. Chem. Soc.* **2001**, *123*, 6714.

(14) (a) Braun, D.; Heeger, A. J. *Appl. Phys. Lett.* **1991**, *58*, 1982. (b) Braun, D.; Moses, D.; Zhang, C.; Heeger, A. J. *Appl. Phys. Lett.* **1992**, *61*, 3092.

(15) Ding, L.; Egbe, D. A. M.; Karasz, F. E. *Macromolecules* **2004**, *37* (16), 6124.

(16) Egbe, D. A. M.; Kietzke, T.; Carbonnier, B.; Mühlbacher, D.; Hörhold, H.-H.; Neher, D.; Pakula, T. *Macromolecules* **2004**, *37*, 8863.

(17) Ding, L.; Karasz, F. E. *J. Appl. Phys.* **2004**, *96*, 2272.

MA040124M